Received: Added at production | Revised: Added at production | Accepted: Added at production
DOI: xxx/xxxx

RESEARCH ARTICLE

Engineering Reports
Open Access

Improving Passenger Safety in Cars Using Novel Radar Signal Processing

Hajar Abedi*[1] | Clara Magnier[2] | George Shaker[3]

[1]System Design Department, University of Waterloo, Ontario, Canada
[2]Department of Biomechanics and Bioengineering, Université de Technologie de Compiegne, Compiegne, France
[3]Electrical and Computer Engineering Department, University of Waterloo, Ontario, Canada

Correspondence
*Hajar Abedi, 200 University Ave W, Waterloo, Canada.
ON N2L 3G1
Email: habedifi@uwaterloo.ca

Funding Information
OCE AVIN

Abstract
We present a novel radar signal processing technique to identify the presence or absence of a living body in a vehicle using a mm-wave frequency-modulated continuous-wave (FMCW) radar. Unlike traditional detection methods which are mostly based on constant false alarm rate (CFAR), our proposed method extracts and monitors the consistent Doppler effects of received signals from the radar antenna. Doppler effects result from the consistent breathing of living bodies over time. The proposed method works in all types of cars without the need for threshold definition for tracking as well as no need for training. Hence, the algorithm is more robust, accurate and fast. We assessed our proposed signal processing with two phantoms mimicking the breathing of children and with adults in a vehicle in various conditions. The system has been proven to be robust in extensive studies over the course of multiple months.

KEYWORDS

mm-wave radar, Doppler effect, radar signal processing.

1 | INTRODUCTION

In 2019, 52 children died of vehicular heatstroke in the United States [1]. This could have been avoided with an occupancy detection system creating a warning signal when someone is left alone in a vehicle. Occupancy detection is currently developed to detect presence of human beings in buildings to save energy, public safety as well as in vehicles. Most of the currently available in-vehicle occupancy detection systems are embedded in seats to monitor the display of airbags or control of the seat belt. In [2], capacitive sensors were used to detect the presence, the type of occupancy on a seat. Capacitive sensors combined with inductive links with switches sensor were also used to detect an occupant [3]. However, the sensors based on an electric field, capacitive and inductive methods have a high false alarm rate. In [4], antenna sensors were also used for occupancy detection in a car where an oscillator supplies a transmitting antenna and the amplitude and phase signals received by the second antenna change if a person sat on the seat. The sensor can detect a person from 3 to 10 cm which might not be feasible to be used in a larger car. Carbone dioxide sensors could have been a possibility but the position of doors and windows, the supply of outdoor air rate and the proximity of the occupants to the sensors affect the signal and reduce the accuracy of the system [5]. Furthermore, video cameras, Passive infrared (PIR) and ultrasound (US) sensors are the some other common sensors developed for occupancy detection in a larger environment but not in vehicles. PIR has been used in [6] to detect the number of persons passing in front of the sensor and the direction of these individuals. One of the major draw backs of PIR sensors is that several layers of clothes could affect the accuracy. Analyzing the room acoustic properties, ultrasonic chirps were used in [7] to estimate the number of occupants in a room. Furthermore, stereovision, a combination of two cameras at a short baseline, was used for the occupancy detection of the cockpit of the car in [8]. The system was tested on images from a database

Received: Added at production | Revised: Added at production | Accepted: Added at production
DOI: xxx/xxxx

including empty seats, children in a booster, standing child and extended passenger. This system only detected the presence in the cockpit of the car, and thus, not feasible for detecting children in the car with three rows. Notably, passive infrared, ultrasounds and video cameras are not a feasible solution due to their limited functionality in different situations and conditions. On the other hand, the use of a radar system is appealing due to its reliable functionality during different conditions, protection of privacy and detection through obstacles. We have been developing an in-vehicle occupancy detection using mm-wave radar technologies [9, 10]. Our purpose in previous works was to count the number of passengers in the car, or to identify the occupied seats. To achieve this goal, we applied machine learning classifiers since we required a high resolution radar to distinguish two persons at the back row of the car. To avoid the need for high resolution radar which is expensive, we applied machine learning to identify the number of passengers in a vehicle.

However, the main purpose of this research is to identify a presence or absence of a living body, especially children, left alone behind the car. In fact, there is no need to know the number of occupants or their location in the car, so no need to distinguish passengers from each other. Hence, we can use the low resolution radar for presence detection without using a machine learning classifier requiring training/testing for each individual car. On the other hand, constant false alarm rate (CFAR) was the most common technique for detection which depends on some predefined parameters and the detection threshold. However, in our application, the size of our targets varied (e.g. infants, pets to adults). Besides, based on our experiment conducted in different cars, different types of cars would have different reflections and multipath effects. Hence, defining a proper detection threshold and parameters of CFAR is extremely difficult as well as decreasing false alarm. A threshold set too low would mean a high false alarm rate and a threshold set too high could cause death (an infant might be missed in the car). Therefore, for the determination of presence or absence, the radar and the signal processing technique must be sensitive enough to detect weak targets with a small signal reflection.

In this paper, we used a low-power and low-cost FMCW radar at 77 GHz to detect the presence of a living body left in the car. We proposed a novel algorithm based on consistent motion of breathing of a living body creating a consistent Doppler effects on radar received signals. This technology will be applied in a car that is not in motion, meaning that radar will start working after the car is stopped. Therefore, we could assume that there is no consistent motion in the car caused by other objects, like a fan or an air conditioner, except a living body. In fact, the only consistent motion in the vehicle stopped would be the consistent chest motion of a living body. Chest motion will create a consistent Doppler effect on the received signal which could be extracted using a Short-Time Fourier Transform (STFT). Based on the consistent Doppler effects and their correlation over time, the presence of a living object will be identified.

2 | SYSTEM DESIGN

2.1 | FMCW RADAR CONCEPT

We used TI mm-wave radar [11] which is Time Division Multiplexed (TDM) MIMO FMCW radar such that the frequency is swept linearly. Unlike traditional pulsed-radar, FMCW radars transmit a frequency-modulated signal called chirp, continuously, to measure range as well as velocity. In a TDM MIMO FMCW radar, a sequence of chirps is sent in a frame from different transmit antennas. Each chirp consisting of a sinusoid signal with swept frequency from (carrier frequency) f_c to f_c +B with the bandwidth of B= f_{max} - f_{min} determines the radar's ability to resolve as separate targets that are close together in range. The received signal then is correlated with the transmit signal creating a beat signal with the frequency of f_b containing information of the illuminated scene. In fact, the time difference (the delay) between the transmitted signal and the received signal (τ) is converted to an instantaneous frequency difference between the

Received: Added at production | Revised: Added at production | Accepted: Added at production
DOI: xxx/xxxx

transmitted and the received chirps. In Figure 1, the transmitted and received signal of FMCW radar and the corresponding beat frequency are shown. Figure 2 (a) and (b) illustrate the chirp and frame structure of the FMCW radar, constructed by defining a sequence of chirps, repectively. There are several defining characteristics of a chirp affecting the operating conditions of the radar in specific ways. The characteristics used to configure a chirp and their effects on the operation of the radar are outlined in Table 1. In FMCW radar, to resolve objects in range, Fast Fourier transform (FFT) processing on the beat signal will be performed such that the frequency of the peaks in the range FFT directly corresponds to the ranges of various objects in the scene. Moreover, in order to obtain the velocity information of an object, a sequence of chirps called a frame will be sent out as shown in Fig. 2 (b). Performing a second series of FFTs (Doppler FFT) across the chirps, the velocity of objects then will be measured.

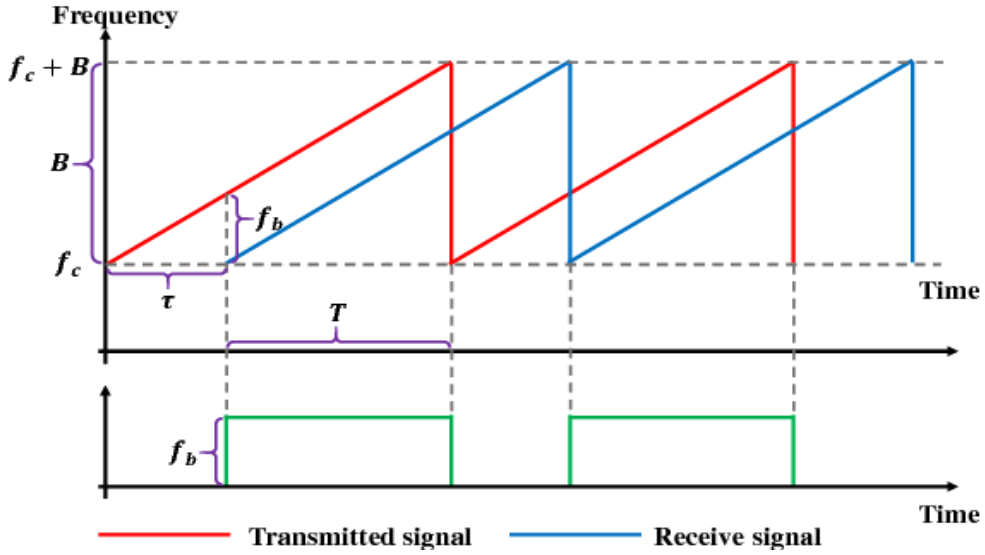

Figure 1: The transmitted/received and the beat signal in FMCW radar.

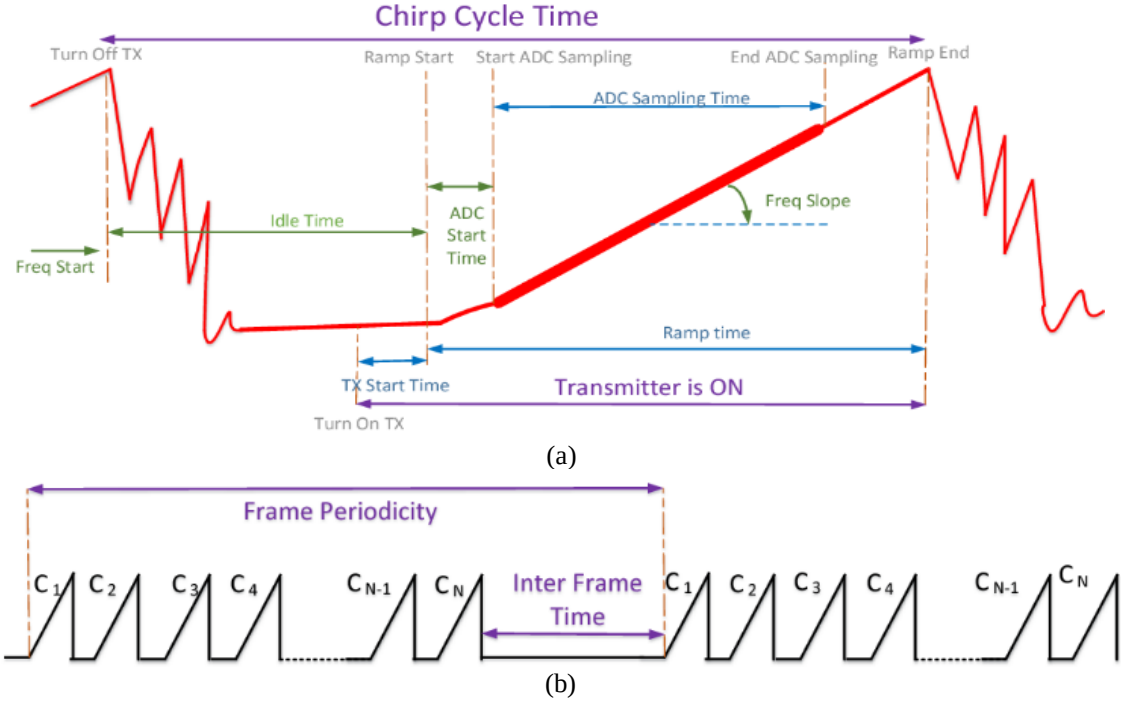

Figure 2: FMWC (a) chirp configuration and (b) frames structure.

Received: Added at production | Revised: Added at production | Accepted: Added at production
DOI: xxx/xxxx

Table 1: chirp characteristics

Characteristic name	***Characteristic description***	***Characteristic effect***
Start Frequency	The frequency the radar signal will start at	Used to determine the bandwidth
Frequency Slope	The slope at which the frequency of the radar is increasing.	Used to determine the bandwidth
Idle Time	The time between the previous chirp finishing and the frequency ramp starting	Must be long enough for the transmitter noise to stop. Should not be too long to increase the frame rate
Transmit Start Time	The time within the chirp where the transmitter is turned on	Should be soon enough before the ramp start time to ensure a smooth start to the ramp
ADC Start Time	The time where the ADC starts sampling	Should be far enough after TX start time such that the ramp has begun increasing. Should be soon enough after the TX start time that the ADC has enough time to collect all its samples
ADC Samples	The number of samples the ADC takes	This value should be large enough for the ADC to collect all the samples in the given time
ADC Sample Rate	The rate at which the ADC takes samples	This value affects the maximum range the radar can detect
Ramp End Time	The time where the frequency ramps finished	Used in bandwidth calculation, and limits the number of ADC samples
Bandwidth	The total frequencies spanned by the chirp	Determines the range resolution

2.2 | PROPOSED ALGORITHM

The main goal of this study was to develop a radar-based technology to save lives by triggering an alarm when children or pets are left alone in vehicles. Our proposed methods are based on these assumptions:

1. The car is not in motion.
2. Doors and windows are locked.
3. No object other than a living body has consistent motion (there is no fan/air conditioner working while the car is stopped)

Our proposed method is based on the fact that the only essential and crucial required information is the presence or absence of a living body in the car. In this regard, we ignored any extra signal processing chain to obtain point cloud information of targets. Moreover, as defining a proper detection threshold that works for all types of cars and all types of living body was difficult or even not possible, we didn't apply the CFAR detection method. Note that depending on the size and type of materials used, number of seats, and type of objects, each individual car has varied reflections and multipath effects creating different detection threshold. Additionally, since the size of infants and pets are extremely small, it may not be accurate or even possible to define proper SNR to distinguish a weak target from noises. Therefore, we based our proposed presence/absence detection algorithm on the most obvious difference between a living object and other targets. Our breathing creates consistent motion resulting in consistent Doppler frequency over time. In fact, since the car is stopped, and windows and doors are also locked, we have no source to create consistent motion inside the car other than a living object, if left behind. The core of our proposed algorithm, thus, is based on Doppler effects created by chest motion o an alive object over time. To start the processing and to avoid any false alarm, the received signals were recorded for T_m minutes, meaning that after the car is stopped, the sensor needs T_m minutes to identify if a living object is left in the

Received: Added at production | Revised: Added at production | Accepted: Added at production
DOI: xxx/xxxx

car. To reduce receiver noise as well as to increase the signal intensity, we illuminated the target scene with as much energy as possible. Since our radar has multiple transmitters and receivers, although there were used to increase angular resolution, we created a virtual channel to improve target detection. The signal processing chain starts with performing FFT on the range of the received chirp samples. At the receiver, the signal is collected and assigned to a virtual channel such that each channel contains the data transmitted and received from and to a unique pair of transceivers. Then, radar cubes containing fast time data related to range and slow time information of frames corresponding to each channel were created over T_L seconds (L number of frames). Coherent accumulation was performed over the virtual channel vector to increase signal intensity. This step was repeated for L number of frames to record more reflected signals of the target over time, or, to increase the observation time. In order to measure the Doppler frequency of a target over time, short-time Fourier transform [13] was performed on received signals according to:

$$Stft(t,f) = \left| \sum_{n=-\infty}^{\infty} w(n)x(t-n)e^{-j2\pi fn} \right|^2 \quad (1)$$

where $w(n)$ is the window function, we used Hamming window centered around zero, and $x(t)$ is the signal to be transformed.

Then, the results of STFT of L frames were accumulated coherently. Finally, to remove the range effect and to have concrete information of all range bins in the car, coherent accumulations over range were performed. The signal processing chain is illustrated in Figure 3. The final result of this chain is the Amplitude-Doppler information over T_L seconds, called observation signal (OS). To identify if a living object is left or not, the signal processing change will be applied on all data recorded for T_m seconds and the results will be stored. Finally, based on the consistent signals created by breathing motion, if a living object is left in the car, all OSs are correlated over T_m seconds, otherwise, they are random data with no correlation. We provide a pseudo code of the proposed presence/absence detection algorithm in Algorithm 1.

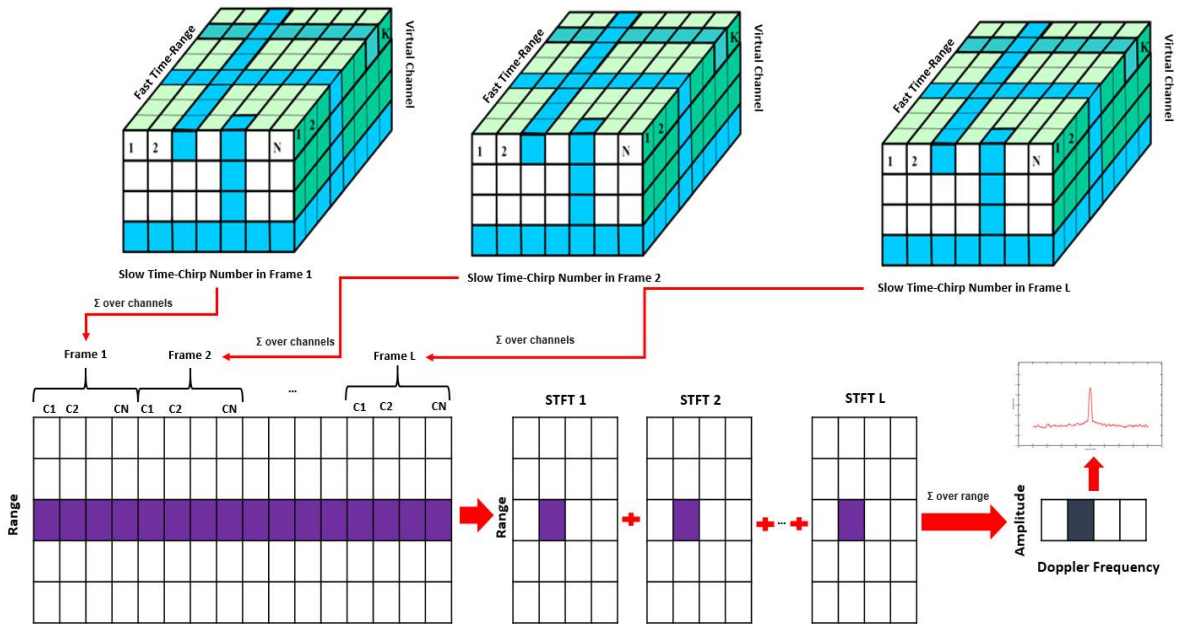

Figure 3: Signal processing flow of proposed in-vehicle algorithm of presence/absence detection of a living body.

Received: Added at production | Revised: Added at production | Accepted: Added at production
DOI: xxx/xxxx

Algorithm 1: The algorithm of Presence/Absence detection of a living body

```
Input  : cube – radar received signals over T_m seconds
Output :  presence or absence of a living body
d=[];
CR=[];
for each new signal S over T_m seconds do
    S=0;
    for i on the number of channels do
        S= S+S_i ;
    end
    ST=o;
    for l on the number of frames (L) do
        ST = STFT (S_l)+ST
    end
    OS=o;
    for k on the number of range bins (K) do
        OS = ST +OS
        d.append (OS)
    end
    for j on number of d-1 do
        CR=corr(d(j), d(j+1))
        CR.append (CR)
    end
    if CR>0 then
        output= Presence  otherwise
        output= Absence
    end
end
```

3 | EXPERIMENTAL RESULTS

3.1 | OUR EQUIPMENT

We used Texas Instrument (TI) mm-wave FMCW chip (AWR1443) [11] for our experiments which operates at 77GHz-81GHz with four receivers (RX) and three transmitters (TX). ADC data (the chirp samples) was captured using DCA1000 EVM board and transferred over the UART interface to a PC [12]. Our measurements were conducted in a 2013 Toyota Sienna with three rows and seven seats. The seat nomenclature is shown in Fig. 4. To find the best location of the radar, the radar was held by a mount with increments every ten degrees, and the mount was placed in two different installation options. The position of the radar in the installation option # 1 and # 2 and the distances to each seat from the radar antennas are shown in Figure 5 (a), (b) and Figure 5 (c), (d), respectively.

To achieve the specific performance of the radar with a visibility range of approximately 2.5m (the length from the radar antennas to the rear of the vehicle did not exceed this number), the chirp configuration in Table 2 was used. The chirp duration was 62 *ms* with an idle time of 250 *ms*, the slope frequency of 60 MHz and the sweeping bandwidth of 3.6 GHz. For the subject, 2 phantoms were used to mimic the breathing motion of a small child as shown in Figure 6. A 3 cm by 3 cm metal plate was programmed to oscillate at variable speeds. The other doll was

Received: Added at production | Revised: Added at production | Accepted: Added at production
DOI: xxx/xxxx

Figure 4: SUV indoor look.

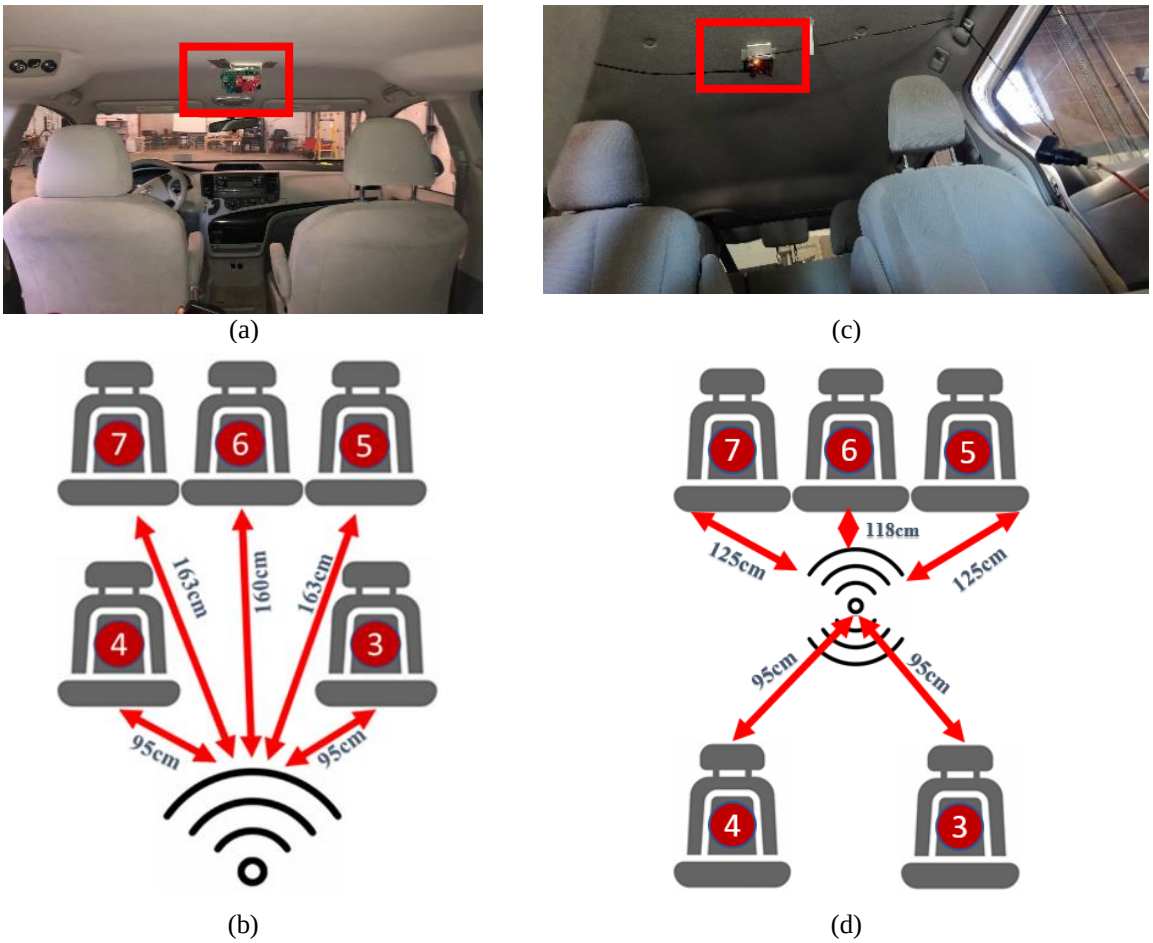

Figure 5: Radar (a) installation option #1 (b) distance to each seat from installation option #1 (c) installation option #2 (d) installation option #2.

purchased to mimic the actual baby, as shown in Figure 6 (c) and (d). The speed used for this experiment resulted in 16-18 cycles per minute, with the motion about 2 cm forwards and backwards. The phantom sat on two different car seats, Figure 6 (a) and (b) show the small doll sat on the booster seat and the rear-facing infant car seat, respectively. Figure 6 (c) and (d) also show the baby doll sat on the booster seat and the rear-facing infant car seat, respectively.

Received: Added at production | Revised: Added at production | Accepted: Added at production
DOI: xxx/xxxx

(a) (b) (c) (d)

Figure 6: Phantoms and car seats used for this project (a) the small doll sat on the booster seat (b) the small doll sat on rear-facing seat (c) the baby doll sat on the rear-facing seat (d) the baby doll sat on the booster seat.

Table 2: Chirp configuration

Parameter	***Specifications***
Idle time (µs)	250
ADC start time (µs)	10
Ramp end time (µs)	60
Number of ADC samples	64
Frequency slope (MHz/µs)	60
ADC sampling frequency (ksps)	2200
Number of chirps per frame	256
Bandwidth (MHz)	3600
Frame periodicity (s)	0.16
Chirp cycle time (ms)	64

3.2 | RESULTS

For the first set of tests, the vehicle was tested with no phantom inside. Figure 7: **STFT results of empty car test (a) at radar installation option # 1 (b) at radar installation option # 2.**Figure 7 (a) and (b) show the STFT result of the recorded signals for both installation options. As seen from Figure 7, since the car was empty and there was no moving object inside, there was no Doppler effect on reflected signals. Note that, in our signal processing, T_m was set to 2 minutes, meaning that the car will be illuminated by radar signals for 2 minutes, the signal will be recorded then the proposed presence/absence detection method will be performed. Moreover, for the observation signal (OS), L=50 frames were selected over T_L=50 × 0.16ms= 8seconds, meaning that the correlation between each successive 8-second observation signal will be applied. In Figure 8, three successive OSs of empty car for both options are provided. As depicted in Figure 8, OS_1, OS_2 and OS_3 of radar received signal at installation option #1 are the results of 3 successive sets which are random signals with no correlation. Similarly, OS_1, OS_2 and OS_3 of radar at installation option # 2 are not correlated. The figures illustrate that if the car is empty, or there is an alive object, the observation signals of different sets are just random signals with no correlation.

To validate the performance and the robustness of the proposed algorithm, various tests were conducted. Since the vehicle used was a seven-seat van, the phantoms were tested in each of the seats behind the first row, seat #3-#7, with different car seats for two radar installation options. Therefore, to yield a concrete result and to measure any possible condition, 5×4×2 different tests were conducted over more than 3 minutes, 5×4×2×3 minutes in total.

Received: Added at production | Revised: Added at production | Accepted: Added at production
DOI: xxx/xxxx

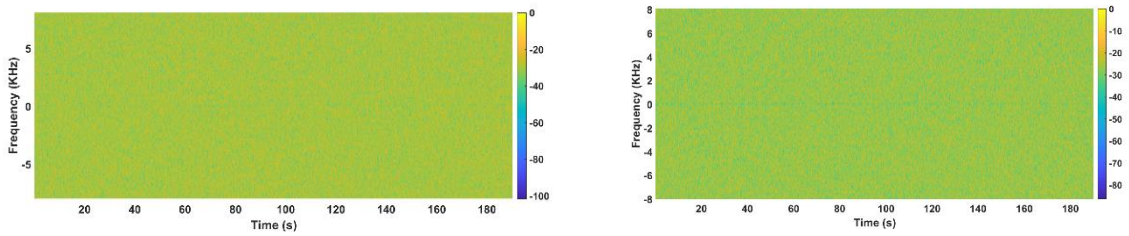

(a) **(b)**

Figure 7: STFT results of empty car test (a) at radar installation option # 1 (b) at radar installation option # 2.

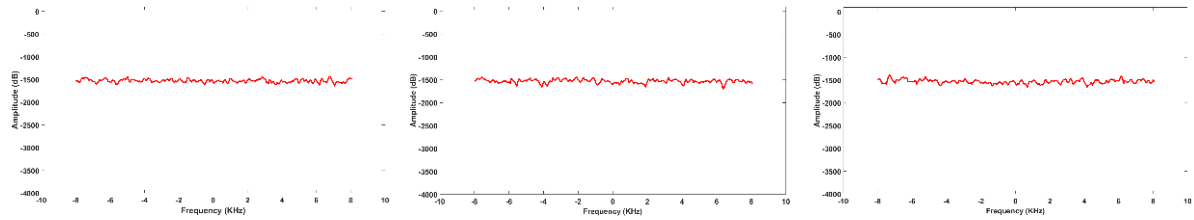

installation option # 1-OS_1 installation option # 1-OS_2 installation option # 1-OS_3

installation option # 2- OS_1 installation option # 2- OS_2 installation option # 2- OS_3

Figure 8: Observation signals of the empty car.

The first set of tests were performed with a human inside the car sitting at all 5 seats for 3 minutes. Figure 9 shows the STFT result of a person inside the car sat on different seats without extra motion except his respiration. As seen, the Doppler effects of breathing are consistent over time and the mm-wave radar can easily detect the tiny motion. Then, OSs were calculated to yield the final concrete answer (absence or presence). OSs of three successive sets of a person sat on seat #4 are provided in Figure 10 for both installations, as an example. Although the amplitude of OSs of installation option #2 were small compared with the amplitude of OSs of installation option #1, all observation signals are correlated together, because of consistent chest motion. The proposed algorithm identified the presence of a person sat on all seats for both installation options correctly.

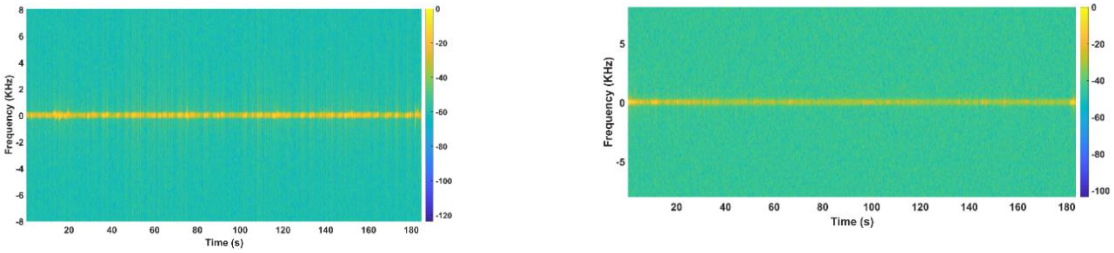

Installation option #1, seat # 3 Installation option #2, seat # 3

Received: Added at production | Revised: Added at production | Accepted: Added at production
DOI: xxx/xxxx

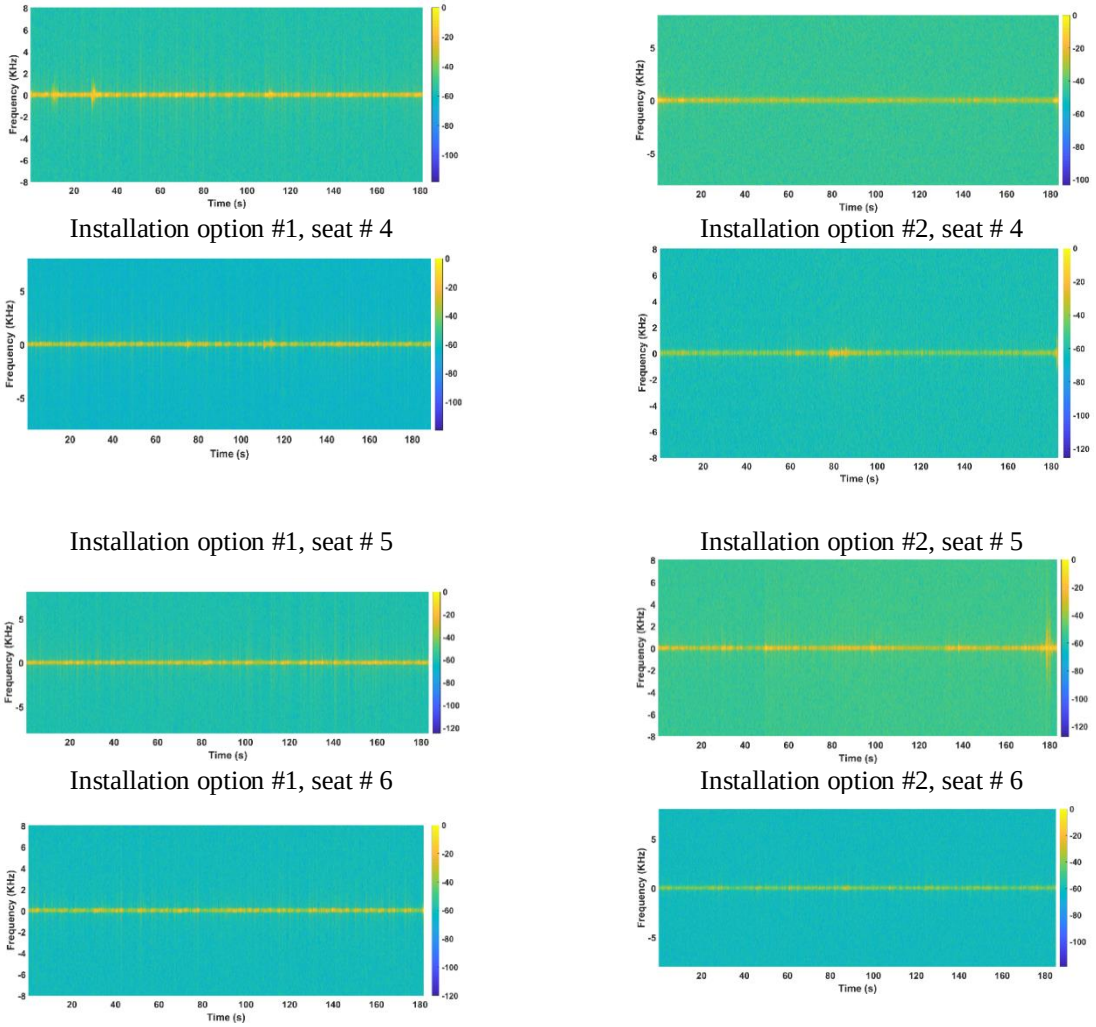

Figure 9: STFT results of the car test occupied by a person.

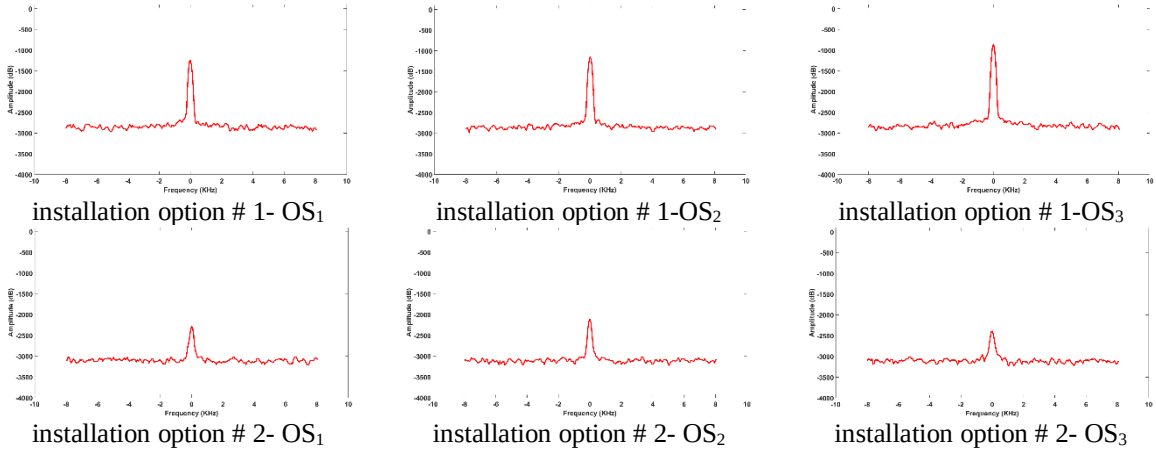

Figure 10: Observation signals of the car occupied by a person, sat on seat #4.

The next set of tests were performed on the car occupied by the small doll sat on both types of car seat, booster and rear-facing seats. The SFTF results of all scenarios are provided in Figure 11. As seen in Figure 11, the radar at both options can clearly detect the doll sat on the booster

Received: Added at production | Revised: Added at production | Accepted: Added at production
DOI: xxx/xxxx

seat. However, for the case of the rear-facing seat, the radar at option #1 was not able to detect the small doll at seat #5 and #7, since the received signal was too weak. To show more details of these scenarios and the radar performance at both installation options, OSs of three successive sets of Option #2 and option #1 of the small doll sat on rear-facing seat at seat #5 are drawn in Figure 12 and 13, respectively. As seen, OSs in Figure 12 are correlated while radar has trouble detecting the motion at Option #1, as shown in Figure 13. The similar tests were conducted for the baby doll created the same results. From these tests, we can conclude that with our proposed algorithm performed on the received signals from the radar installed at Option #2, we can identify the presence of a living body inside the car without any false alarm and missed object.

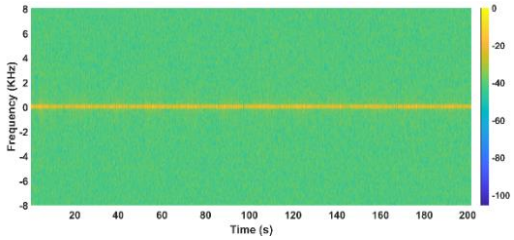

Installation option #1, seat # 3- the booster seat

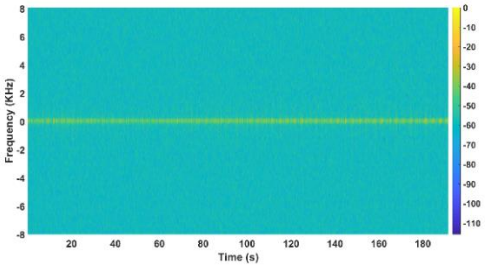

Installation option #2, seat # 3- the booster seat

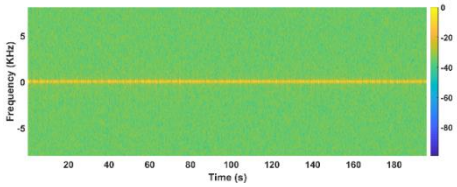

Installation option #1, seat # 4- the booster seat

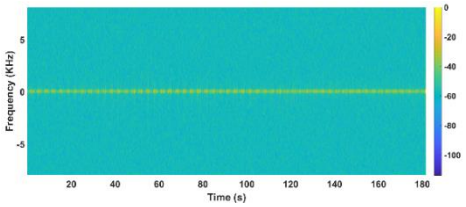

Installation option #2, seat # 4- the booster seat

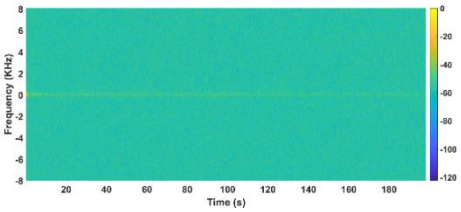

Installation option #1, seat # 5- the booster seat

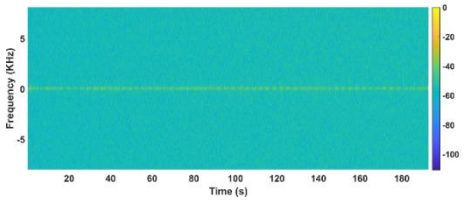

Installation option #2, seat # 5- the booster seat

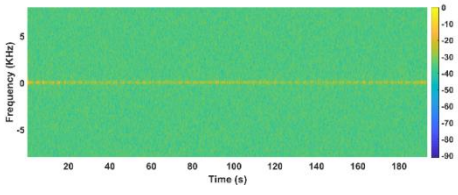

Installation option #1, seat # 6- the booster seat

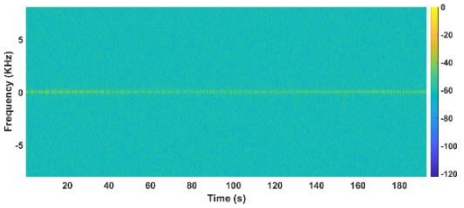

Installation option #2, seat # 6- the booster seat

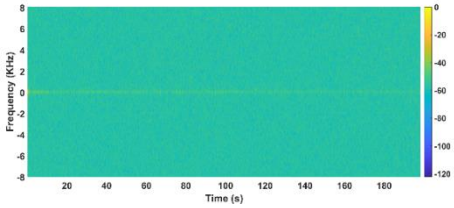

Installation option #1, seat # 7- the booster seat

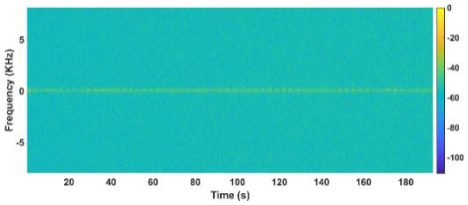

Installation option #2, seat # 7- the booster seat

Received: Added at production | Revised: Added at production | Accepted: Added at production
DOI: xxx/xxxx

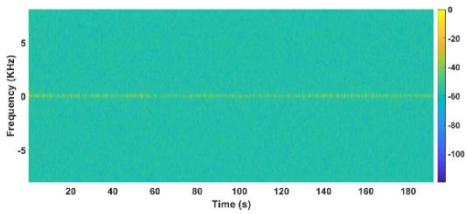

Installation option #1, seat # 3- the rear-seat

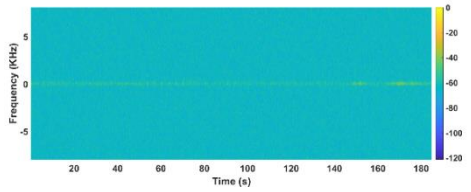

Installation option #2, seat # 3- the rear-seat

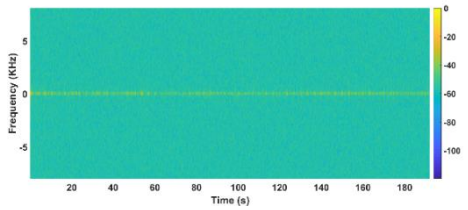

Installation option #1, seat # 4- the rear-seat

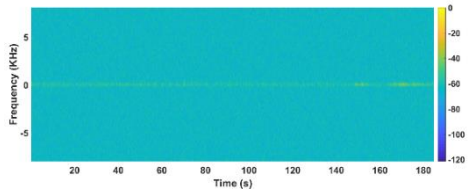

Installation option #2, seat # 4- the rear-seat

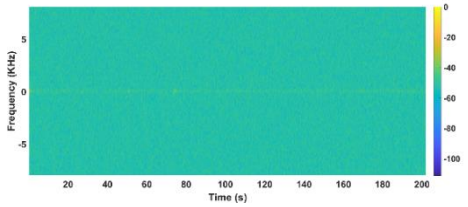

Installation option #1, seat # 5- the rear-seat

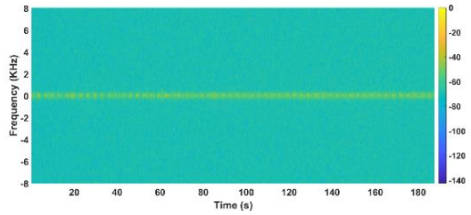

Installation option #2, seat # 5- the rear-seat

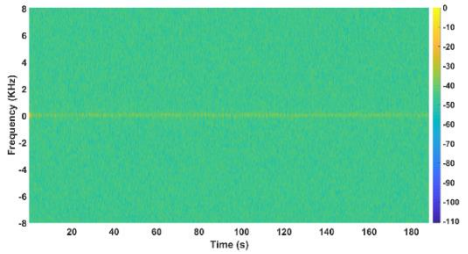

Installation option #1, seat # 6- the rear-seat

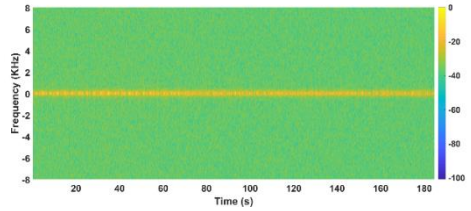

Installation option #2, seat # 6- the rear-seat

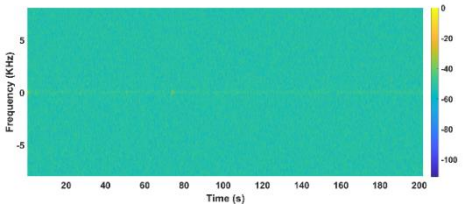

Installation option #1, seat # 7- the rear-seat

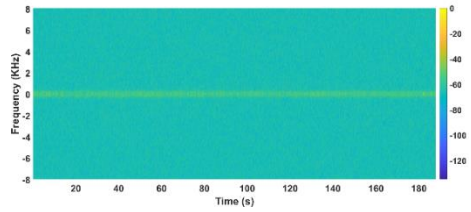

Installation option #2, seat # 7- the rear-seat

Figure 11: STFT results of the car test occupied by the small doll.

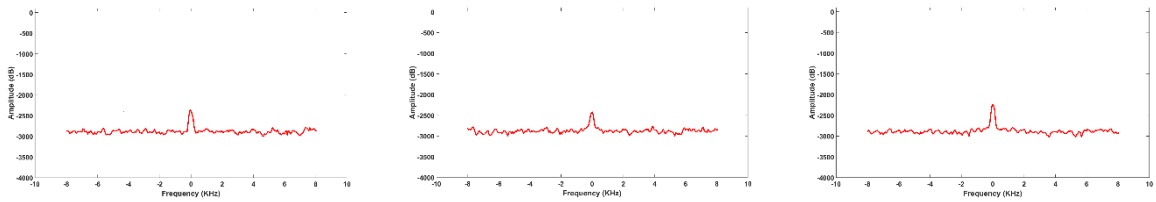

installation option # 2- OS_1 installation option # 2-OS_2 installation option # 2-OS_3

Figure 12: Observation signals of the car occupied by the small doll, sat on rear-facing seat at seat #5.

Received: Added at production | Revised: Added at production | Accepted: Added at production
DOI: xxx/xxxx

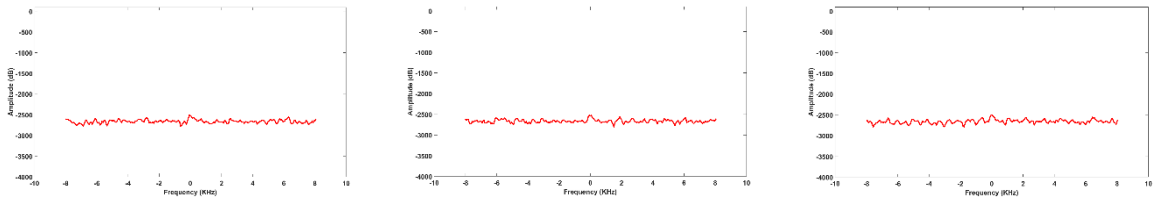

installation option # 1- OS_1 installation option # 1- OS_2 installation option # 1- OS_3

Figure 13: Observation signals of the car occupied by the small doll, sat on the rear-facing seat at seat #5.

For more complicated and challenging scenarios, the dolls were placed on the floor of the car (under seats). The same process was applied, and the proposed algorithm clearly identified the presence of the doll inside the car. To show how accurately radar can detect the presence of the doll in the car, even under the seat, the STFT results of the baby doll under the seat #7 for both installation options are provided in Figure 14. The Doppler effects of the doll's motion was detectable over time. Performing the proposed algorithm, the results yield 100% accuracy in detecting the presence of the dolls under seats.

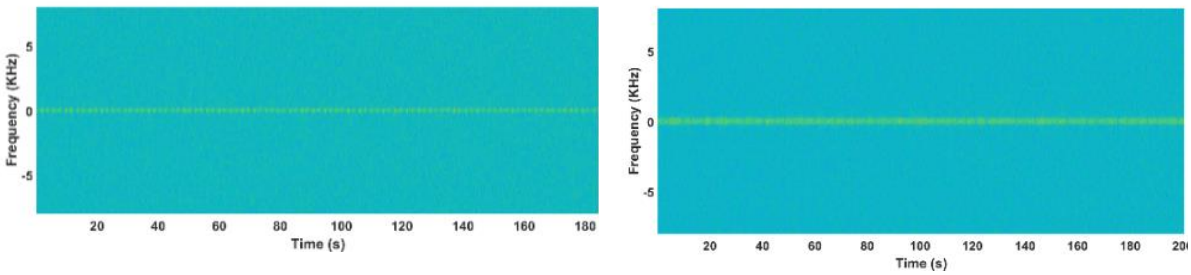

Installation option #1, seat # 7 Installation option #1, seat # 7

Figure 14: STFT results of the car test occupied by the baby doll on the floor (under the seat #7).

In addition to the tests mentioned above, a set of tests was performed when clutter was present in the vehicle. The clutter was added to mimic unexpected objects that would change how the signal behaved inside the vehicle. Figure 15 (a) shows an example of the clutter added to the car without any living body while Figure 15 (b) shows the car with clutter and a small doll. A test was run when there was no phantom in the vehicle to see the effect of clutter on a vehicle with no person, and then the phantom was placed in seat #7 with the booster seat. The STFT result of the car with cluttered added without any phantom inside is shown in Figure 16 (a). As depicted, since the clutter had some sudden motions, the STFT result shows some spot (represented by red rectangles). However, the proposed signal processing clearly identified them as an absence, since the motion was not consistent over observation time. On the other hand, the STFT results of the car with both clutter and the phantom in Figure 16 (b) clearly shows the consistent motion of the doll. Therefore, from these different sets of tests, our proposed algorithm has been proved.

Received: Added at production | Revised: Added at production | Accepted: Added at production
DOI: xxx/xxxx

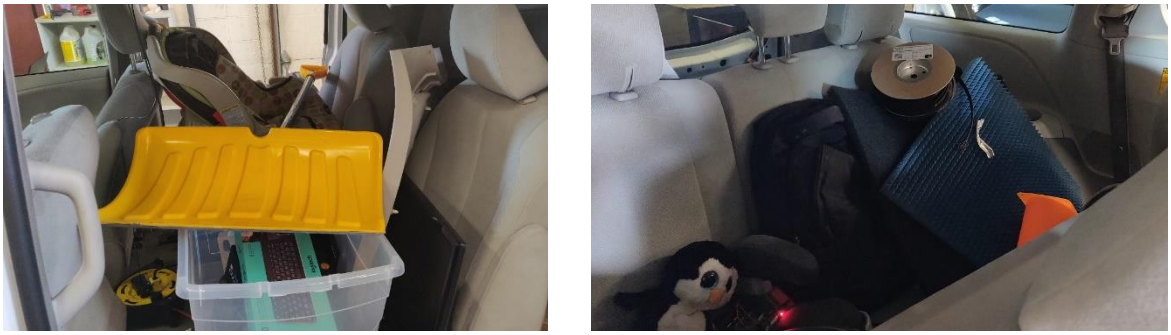

(a) (b)

Figure 15: The car with clutter added (a) with no phantom inside (b) with the phantom sat on seat #7.

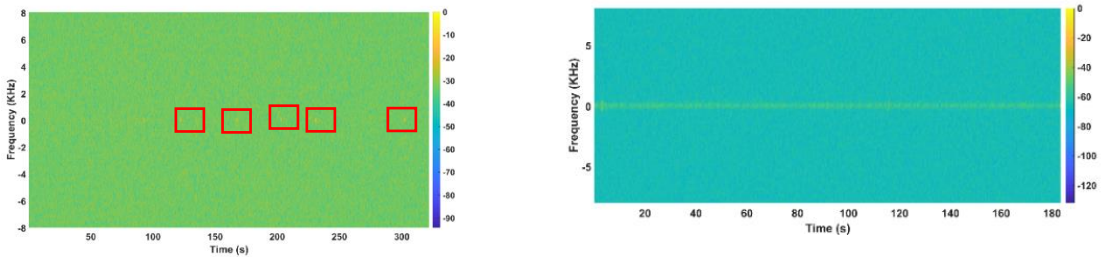

(a) (b)

Figure 16: STFT results of the car test with clutter added (a) without the phantom (b) with the phantom sat on seat #7.

4 | CONCLUSION

The aim of this paper was to determine the feasibility of radar technology to detect the presence of a small child using the movement of their chest caused by breathing. To mimic a small child, a phantom with an oscillating metal plate was placed in various car seats and then tested in each seat of the two back rows of a minivan. A novel radar signal processing technique is based on a consistent movement of a living body's chest which creates consistent Doppler over time was proposed. Then the plots of observation signals of chest motion were extracted and compared with each other over time. The results shows that if there was no phantom in the vehicle, these observation signals had no correlation with each other over time. However, observation signals extracted from a phantom and a person was shown to be correlated with each other over time. The proposed algorithm was proved reliable enough to detect the phantoms at all scenarios and under seats as well as to detect humans with no false alarm.

ACKNOWLEDGEMENTS

The authors wish to acknowledge the support of the National Sciences and Engineering Research Council of Canada as well as the Ontario Centres of Excellence. This study was funded by the OCE Autonomous Vehicle Innovation Network.

CONFLICT OF INTEREST

The authors declare no potential conflict of interest.

Received: Added at production | Revised: Added at production | Accepted: Added at production
DOI: xxx/xxxx

1 **REFERENCES**
2

[1] «Heatstroke Death of Children in Vehicle,» [Online]. Available: https://noheatstroke.org/. [Access the 21 January 2020].

[2] B. George, H. Zangl, T. Bretterklieber and G. Brasseur, «Seat Occupancy Detection Based on Capacitive Sensing.,» *IEEE Transactions on Instrumentation and Measurement*, pp. 1487-94., 2009 May.

[3] B. George, H. Zangl, T. Bretterklieber and G. Brasseur, «A Combined Inductive–Capacitive Proximity Sensor for Seat Occupancy Detection.,» *IEEE Transactions on Instrumentation and Measurement*, pp. 1463-70., 2010 May.

[4] H. Sterner, W. Aichholzer and M. Haselberger, «Development of an Antenna Sensor for Occupant Detection in Passenger Transportation.,» *Procedia Engineering*, pp. 178-83, 2012.

[5] J. Yang, M. Santamouris and S. Lee, «Review of occupancy sensing systems and occupancy modeling methodologies for the application in institutional buildings,» *Energy & Buildings*, pp. 344-9., 2016 June .

[6] P. Zappi, E. Farella and L. Benini, «Enhancing the spatial resolution of presence detection in a PIR based wireless surveillance network,» *IEEE Conference on Advanced Video and Signal Based Surveillance*, 2007.

[7] O. Shih and A. Rowe, «Occupancy Estimation Using Ultrasonic Chirps.,» *Proceedings of the ACM/IEEE Sixth International Conference on Cyber-Physical Systems.*, pp. 149-58, 2015.

[8] M. Devy, A. Giralt and A. Marin-Hernandez, « Detection and classification of passenger seat occupancy using stereovision.,» *Proceedings of the IEEE Intelligent Vehicles Symposium, October 2000.*

[9] M. Alizadeh, H. Abedi and G. Shaker, «Low-cost low-power in-vehicle occupant detection with mm-wave FMCW radar,» *IEEE Sensor*, 2019.

[10] H. Abedi, L. Shenghan, S. Ding, C. Magnier, M. Bacani and G. Shaker, «On the Use of Low-Cost Radars and Machine Learning for In-Vehicle Passenger Detection», *5th Annual Conference on Vision and Intelligent Systems*, 2019.

[11] AWR1443 Single-Chip 76-GHz to 81-GHz Automotive Radar Sensor Integrating MCU and Hardware Accelerator | TI.com. [Online]. Available: http://www.ti.com/product/AWR1443

[12] «Real-time data-capture adapter for radar sensing evaluation module,» [Online]. Available: http://www.ti.com/tool/DCA1000EVM .

[13] C. Victor C, M. William J and T. David, «Radar micro-Doppler signatures: processing and applications,» *The Institution of Engineering and Technology*, 2014.

3